ANSF APPLIED AND NATURAL SCIENCE FOUNDATION

Journal of Applied and Natural Science
15(4), 1667 - 1678 (2023)
ISSN : 0974-9411 (Print), 2231-5209 (Online)
journals.ansfoundation.org

Research Article

Application of Revised Universal Soil Loss Equation (RUSLE) model for the estimation of soil erosion and prioritization of erosion-prone areas in Majuli Island, Assam, India

Arpana Handique
Centre for Studies in Geography, Dibrugarh University, Dibrugarh, India
Praduyt Dey*
Department of Geography, Rajiv Gandhi University, Itanagar, Arunachal Pradesh, India
Santanu Kumar Patnaik
Department of Geography, Rajiv Gandhi University, Itanagar, Arunachal Pradesh, India

*Corresponding author. E-mail: praduytd25@gmail.com

Article Info
https://doi.org/10.31018/jans.v15i4.5176
Received: September 28, 2023
Revised: December 8, 2023
Accepted: December 12, 2023

How to Cite

Handique, A. *et al.* (2023). Application of Revised Universal Soil Loss Equation (RUSLE) model for the estimation of soil erosion and prioritization of erosion-prone areas in Majuli Island, Assam, India. *Journal of Applied and Natural Science*, 15(4), 1667 - 1678. https://doi.org/10.31018/jans.v15i4.5176

Abstract
Soil erosion is a serious issue, causing loss of agricultural productivity, increase in sediment deposit in the riverbeds, and damage to the ecological balance of the affected areas. Proper assessment of the soil erosion rate is essential for managing natural resources. The present study employs a GIS-based RUSLE (Revised Universal Soil Loss Equation) model to estimate annual soil loss in Majuli River Island of Assam, India. Annual average rainfall, soil properties, topographic characteristics, and LULC were taken as inputs to identify the soil erosion susceptible areas. The result revealed that annual soil loss of the study area ranges between 0 to 711 t ha^{-1} yr^{-1}, with a mean annual soil loss of 23.02 t ha^{-1} yr^{-1}. The entire region was classified into six soil loss severity classes, around 90 % of the area was found to be very slightly affected (< 5 t ha^{-1} yr^{-1}) by soil erosion, around 5 % slightly affected (5 – 10 t ha^{-1} yr^{-1}), roughly 3% moderately affected (10 – 20 t ha^{-1} yr^{-1}), around 1% moderate high (20 – 40 t ha^{-1} yr^{-1}), nearly 0.3 % area affected severely (40 -80 t ha^{-1} yr^{-1}) and very severely affected areas (> 80 t ha^{-1} yr^{-1}) contributes 0.1 %. A total of six priority levels of conservation were demarcated village-wise; priority level I requires immediate attention, and so on. The research outcome can help effectively implement conservation and management practices to check soil erosion in the study area.

Keywords: Geographical Information System (GIS), Majuli Island, Remote Sensing, Revised Universal Soil Loss Equation (RUSLE) Soil Erosion.

INTRODUCTION

Soil erosion is a serious problem worldwide, mostly where fluvial processes are pro-active. It is the disintegration and removal of topsoil due to the combined effect of rainfall and surface runoff affecting the soil's nutrition level, thereby affecting any region's agricultural productivity. It is estimated that the average rate of soil erosion throughout the world is roughly between 12 to 15 tons/ha/year (Biggelaar *et al*., 2003; Buraka *et al*., 2022), which implies 0.96 to 1.2mm of soil loss from the land surface every year (Food and Agriculture Organization, 2019). In India, out of 328.8 million hectares of the total land surface, 94 million hectares are affected by soil erosion caused by water, 16 million hectares are affected by acidification, 14 million hectares by flooding,9 million hectares by wind erosion, 6 million hectares are affected by salinity and 7 million hectares are affected by a combination of factors (Bhattacharyya *et al*., 2015)

Soil erosion results from several factors, including soil types, rainfall intensity, topographic conditions, and anthropogenic land use (Makhdumi *et al*., 2023). The slope characteristics influence run-off mechanisms, viz. higher slope angle increases surface run-off and limits infiltration (Barman *et al*., 2022; Makhdumi *et al*., 2023). Soil physical properties play an important role in holding the soil particles together viz., weaker soil types comprised of silt are more prone to erosion as the soil lacks the strength to bind the soil particles together owing to high runoff rate, while sandy and clayey soil are less prone to soil erosion (Ghosh *et al*., 2022). Land use and land cover changes such as alteration in agricultural practices, clearing of the forest, etc. have accelerated the rate of soil erosion (Guo *et al*., 2019).

Several research studies have identified that soil loss is mainly due to water erosion which is aggravated by inadequate land use and management practices such as unscientific tillage and agriculture practices (Bhatt *et al*., 2020). Soil erosion devastates the nutrient-rich topsoil as it exposes the impermeable sub-surface soil, reducing the soil water content (Zhao *et al*., 2019). In a developing country like India, where agriculture is the backbone of the economy, the impact of soil loss, particularly, the loss of top fertile soil, has a huge effect on agricultural output, land use intensity, and cropping patterns, all of which have significant environmental and economic consequences (Rajbanshi and Bhattacharya, 2020). Apart from affecting agricultural productivity, soil erosion increases the siltation of the rivers, reservoirs, and wetlands leading to disasters like floods and drought, which threaten the ecology of the affected areas (Jamal *et al*., 2022).

In recent decades, research communities across the globe have mainly focused on estimating soil erosion and sediment yield in river basins using remote sensing and GIS techniques (Issaka and Ashraf, 2017). The conventional soil erosion assessment method requires more time and money, especially when the study area is large, like a district block (Srinivas *et al*., 2002; Jiang *et al*., 2015; Karamage *et al*., 2017). Here, effective modeling aided with remote sensing and GIS can provide useful information about the current erosional processes and future predictions.

In the year, 1968 Wischmeier and Smith developed the Universal Soil Loss Equation (USLE) model that can predict soil erosion from cropland, which later became very popular throughout the world (Bhattarai and Dutta, 2007; Kouli *et al*., 2009; Demirci and Karaburun, 2012). In the early 1990s, the basic USLE model was updated and computerized to create an erosion prediction tool that can be integrated with remote sensing and geographic information systems and was called the Revised Universal Soil Loss Equation (RUSLE) (Demirci and Karaburun, 2012; Fu *et al*., 2005; Renard *et al*., 1997; Yue-Qing *et al*., 2008). The RUSLE model became popular among researchers as it can be practically used for predicting soil loss due to its capacity to include various control management and practices with limited data requirements (Sujatha and Sridhar, 2018). The model can effectively predict the average annual rate of soil erosion based on data related to rainfall, soil, topography, cropping system, and soil management practices (Ayalew *et al*., 2020; Pham *et al*., 2018; Wischmeier and Smith, 1978). It considers the factors namely, rainfall erosivity (R), soil erodibility (K), topography (LS), cover and management (C), and support practice (P) (Ayalew *et al*., 2020).

Majuli, the world's largest inhabited river island has been greatly affected by soil erosion after the 1950 earthquake. In 1950, due to a severe earthquake, the south bank of the river Brahmaputra was affected enormously, resulting in the construction of protective measures for bank erosion near the Kokilamukh area, leaving the north bank in Majuli unprotected (Sankhua *et al*., 2005). The riverbed was affected by the deposition of silt and alluvium altering the flow dynamics and resulting in severe erosion (Goswami, 2011). The present study aimed to apply the RUSLE model in combination with geospatial technology, mainly remote sensing and GIS, to determine the rate of soil erosion in Majuli Island, Assam, which is considered sensitive to land degradation. It also intended to identify the priority areas of soil conservation that may help the planners and decision-makers successfully implement soil management practices and ensure sustainable development.

MATERIALS AND METHODS

Description of the study area

The study area, Majuli Island is located in Assam and is the only island district in India. It is situated between 26° 40′ N to 27° 10′ N latitude and 93° 40′ E to 94° 40′ E longitude (Fig. 1). The area is a fluvially originated delta formed by the gradual deposition of sediments by a large number of north and south bank tributaries of the river Brahmaputra. Maujli Island is about 94.83 km long and has an average width of about 10-15 km with a total geographic area of about 935.76 sq. km.

The region's highest elevation is 84.5 above sea level (Dutta *et al*., 2010). The Subansiri River bounds the Island on the northwest, the Khertatia Suti on the northeast, and the main Brahmaputra River on the south and southwest (Dutta *et al*., 2010). The Brahmaputra is a highly braided river. Its channel near Majuli Island constantly shifts every year, especially towards the north, which increases the rate of soil erosion and flood occurrence, posing a huge threat to the inhabitants and their cultural landscapes.

Data collection and sources

The study used various geospatial datasets acquired from different sources (Table 1). The data for performing the RUSLE model comprised rainfall, soil, digital elevation model (DEM), and satellite images. Cloud-free Landsat 8 OLI satellite image path 135/ row 41 was acquired on 20.08.2023 to extract information regarding land cover management and practices and SRTM 1 Arc-Second DEM (30 m resolution) was acquired on 30.06.2023 to analyse the topographic influ-

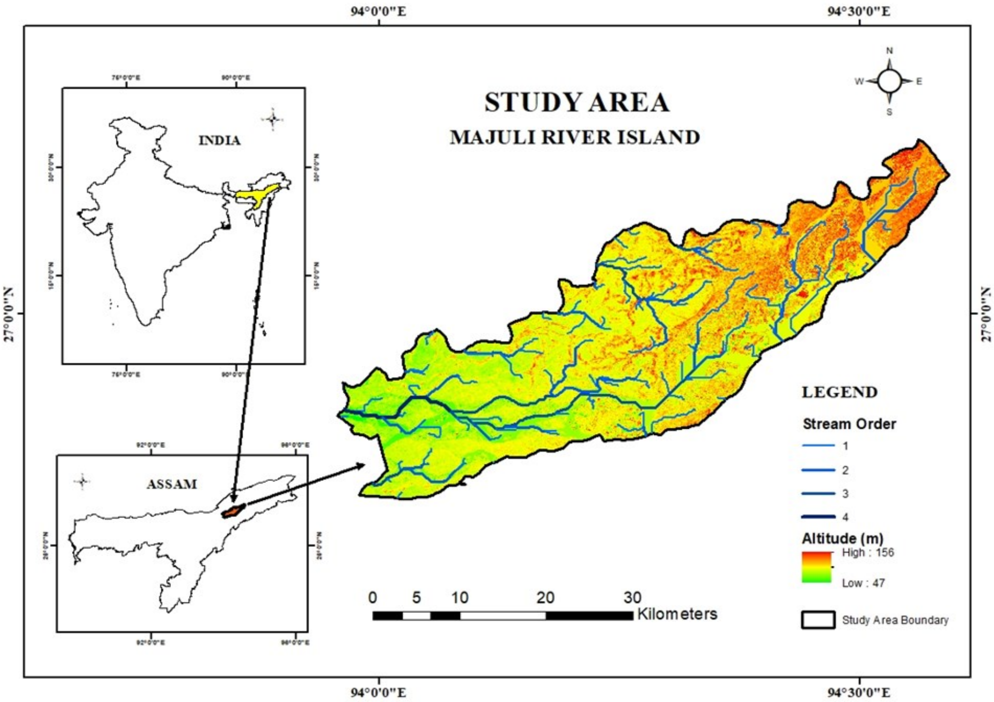

Fig. 1. *Location of the study area*

ence on soil erosion. Both Landsat image and SRTM DEM were collected from Earth Explorer (United States Geological Survey). The gridded average annual rainfall data, with a spatial resolution of 5 km for a period of 41 years (1981- 2022), used for the analysis of rainfall erosivity, was downloaded from CHIRPS (Climate Hazards Center InfraRed Precipitation with Station data) on 01.07.2023. Standardized soil profile data of the world that provides information about soil properties, especially sand, silt clay content, and organic carbon for the analysis of soil erodibility was acquired on 20.08.2023 from the World Soil Information Service developed and maintained by ISRIC, WDC-Soils. The map of the administrative boundary was acquired from the Socioeconomic Data and Applications Center from the archive developed by Meiyappan *et al*. (2018). Fig. 2. shows the methodological framework adopted for the estimation of soil erosion in Majuli District, Assam, India.

Development of the RUSLE Model factors for soil erosion estimation

The Revised Universal Soil Loss Equation (RUSLE) model considers mainly five factors, rainfall erosivity factor (R), soil erodibility factor (K), slope length and steepness factor (LS), cover management factor (C) and conservation practice factor (P) for the estimation of the average annual soil loss (A) (Renard *et al*., 1997) and can be expressed as

$$A = R \times K \times L \times S \times C \times P \quad (1)$$

where, A = average annual soil loss (t ha−1 yr−1), R = rainfall erosivity factor (MJ mm ha−1 h −1, yr−1), K = soil erodibility factor (t h MJ−1 mm−1), LS = slope-length and slope steepness factor (dimensionless), C = land management factor (dimensionless), and P = conservation practice factor (dimensionless).

Rainfall erosivity factor (R)

The rainfall erosivity factor (R) highlight the erosive power of rainfall which evaluate the impact of raindrops in the form of kinetic energy and also helps in predicting the rate and amount of surface run-off during a precipitation event (Ghosal & Bhattacharya, 2020). Wischmeier and Smith (1957) in their work have mentioned that the rainfall erosivity (R) factor is the product of the kinetic energy of a rainstorm and its maximum 30-minute intensity, which is expressed as EI_{30} and identified the method to give the most reliable estimate of soil erosion. However, such data namely, the kinetic energy of rainfall and rainfall intensity (EI_{30}) is not available for the study area. Therefore, the empirical equation (Singh,1981) was used to estimate the Rainfall erosivity (R) factor in the Indian context. The equation is expressed as,

$$R = 79 + 0.363\ \mathrm{AAP} \quad (2)$$

where 'R' is the rainfall erosivity factor, 'AAP' is the average annual precipitation in mm. Rainfall erosivity (R) is expressed in MJ mm ha^{-1} h^{-1} yr^{-1}. The higher R-factor value signifies more power of raindrops to erode the topsoil. Average annual rainfall data for a period of 41 years (1981- 2022) was used to generate a rainfall map in the ArcGIS environment using Inverse Distance Weighting (IDW), a popular interpolation tech-

Table 1. The datasets used in the study and their respective sources

Dataset	Source	Date of acquisition
Satellite data (Landsat 8)	http://earthexplorer.usgs.gov/	Data acquired on 20.08.2023
SRTM DEM	http://earthexplorer.usgs.gov/	Data acquired on 30.06.2023
Soil data	http://soilgrids.org	Downloaded on 20.08.2023
Rainfall data	https://data.chc.ucsb.edu/products/CHIRPS-2.0/	Downloaded on 01.07.2023
Administrative boundary	https://sedac.ciesin.columbia.edu/	Data acquired on 16.07.2023

nique, and consequently, applying Eq. (2) in a raster calculator, the R factor map was generated.

Soil Erodibility Factor (K)

The soil erodibility (K) factor indicates the soil loss rate per rainfall erosion index unit measured on a standard plot determined by the inherent soil properties (Parysow *et al*., 2003). It relies on soil and/or geological characteristics, such as parent material, structure and texture (*Ditzler et al*., 1951), organic matter content, and porosity (Schwab *et al*., 1994). The properties of the top soil play a decisive role in soil erosion. The values can range from 0 to 1, higher K factor values indicate higher probability of soil erosion and vice-versa (Mohapatra, 2022).

The K factor was estimated using the soil type map acquired from the World Soil Information Service Snapshot- 2019 (Batjes *et al*., 2020), which was extracted according to the study area in ArcGIS software. The physical properties of each soil type, mainly silt, sand, and clay as well as the organic matter was extracted following the soil texture classification scheme (Groenendyk *et al*.,2015)which was used to generate the K factor values using a formula adopted from published literature (Sharpley and Williams, 1990).

$$K = Fcsand \times Fsi - cl \times Forgc \times Fhisand \times 0.1317 \quad (3)$$

$$Fcsand = \left[0.2 + 0.3.exp\left(-0.256.SAN\left(1 - \frac{SIL}{100}\right)\right)\right] \quad (4)$$

$$Fsi - cl = \left[\frac{SIL}{CLA + SIL}\right]^{0.3} \quad (5)$$

$$Forgc = \left[1.0 - \frac{0.25\,C}{C + exp(3.72 - 2.95C)}\right] \quad (6)$$

$$Fhisand = \left[1.0 - \frac{0.70\,SN_1}{SN_1 + exp(-5.51 + 2.95\,SN_1)}\right] \quad (7)$$

where, SAN, SIL and CLA represents percentage (%) sand, silt and clay, respectively; C is the organic carbon content; and SN1 is sand content subtracted from 1 and divided by 100, Fcsand indicates a low soil erodibility factor for soil with coarse sand and a high value for soil with little sand content, Fsi-cl reflects a low soil erodibility factor with high clay to silt ration, Forgc is the factor that reduces soil erodibility for soil with high organic content, whereas, Fhisand is the factor that reduces soil erodibility for soil with extremely high sand content.

Slope length and Steepness factor (LS)

The effect of terrain and topography on soil loss is reflected by the slope length (L) and slope steepness (S) factors (Chang *et al*., 2016). The cumulative run-off and its velocity contributing to soil erosion are the outcome of increased slope length and steepness (Ghosal and Bhattacharya, 2022). The L and S were generated using SRTM DEM (2023) data at 30 m resolution downloaded from Earth Explorer, USGS. The LS factor was thus calculated using ArcGIS in a raster calculator following the equation suggested by Wischmeier & Smith (1957).

$$LS = \left(\frac{\lambda}{\Psi}\right)^2 .(0.065 + 0.046s + 0.0065s^2) \quad (8)$$

Where λ is the flow path length (m or feet), which is expressed as λ = (flow accumulation × cell size), the value of Ψ is 22.13 for SI units as the (LS) factor is the ratio of soil loss per unit area from a field slope to that from a 22.13 m length. S is average slope (%), m = 0.2 for s < 1, 0.3 for 1 ≤ 3, 0.4 for 3 ≤ s < 5, 0.5 for 5 ≤ s < 12 and 0.6 for s ≥ 12%.

Cover and management Factor (C)

The vegetation cover of any place plays a very significant role in soil erosion as it reduces the impact of raindrop energy on soil surface (Benkobi *et al*., 1994; Ghosal and Bhattacharya, 2022). The C factor used in RUSLE equation depicts the influence of land cropping and terrestrial vegetation management in the rate of soil erosion (Renard *et al*., 1996). The C factor value ranges between 0 to 1 where, 0 indicates very strong cover effects and 1 indicates no cover effect and the respective land surface treated as barren land and vulnerable (Erencin, 2000). Hence, if the land use and land cover of an area comprises of highest percentage of vegetation and crop field, the impact of C factor on soil erosion is nominal (Ganasri and Ramesh, 2016). The land use and land cover map prepared in ArcGIS using supervised image classification was used to derive the crop

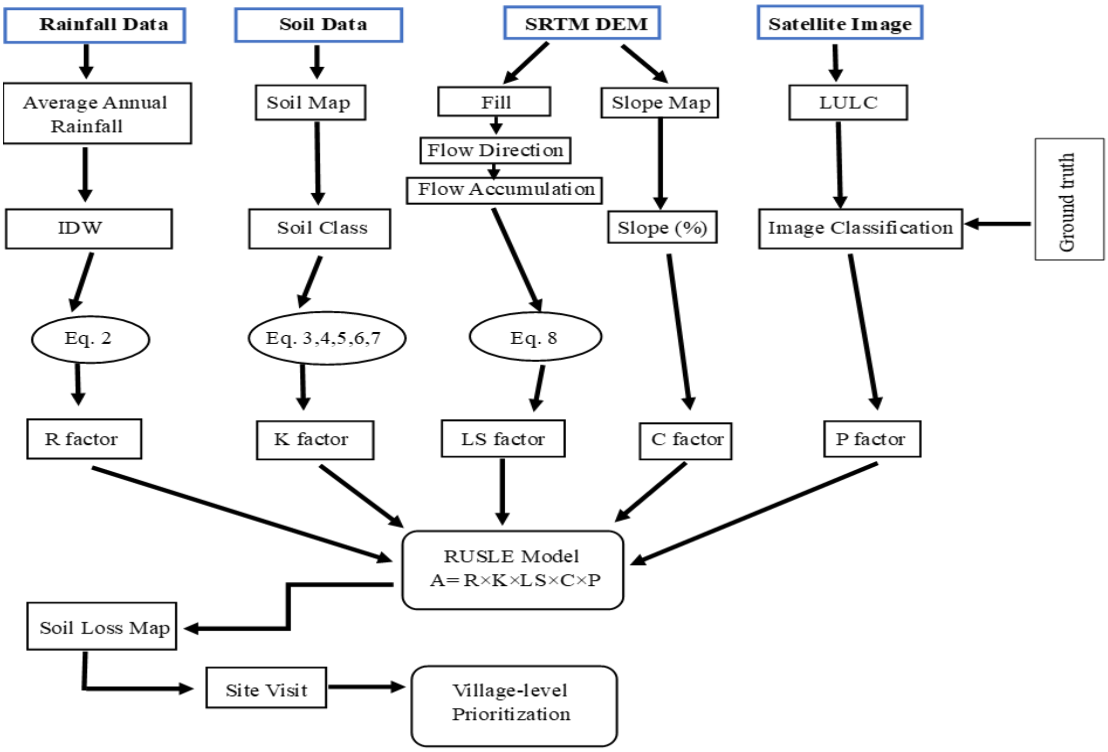

Fig. 2. *Flow chart showing the methodology adopted*

management (C) factor for the study area. The LULC were classified into six feature classes according to the ground information. The C value was assigned to each class accordingly. (United States Soil Conservation Service, 1972; Wischmeier and Smith, 1978; Pandey *et al*., 2007).

Conservation support practice factor (P)

The conservation or support practice factor (P) shows the effects of conservation practices that will decrease the rate and amount of run-off, and, thus, reduce the rate of soil erosion (Ghosal and Bhattacharya, 2022). Several studies suggest that the P factor is directly proportionate to soil loss for a particular support practice in an area with an upward and downward slope, tillage practice, contour farming (Wischmeier and Smith,1957; Renard *et al*.,1997). The Conservation (P) factor ranges from 0 to 1, where the value near to 0 indicates the presence of conservation practices like, contour cropping, built-up land and the areas devoid of any conservation practices (barren areas, grasslands) are given a value of 1.

Estimation of Annual Soil Loss and identification of the priority area of conservation

The input data, namely, R, K, LS, C, and P factors in raster format were integrated and overlayed in ArcGIS using eq. 1 in the raster calculator to generate the final soil erosion estimation map with a spatial resolution of 30 meters for the study area. The soil erosion map was categorized into six classes namely, less than 5 t ha−1 yr−1 (Very slight), 5 – 10 t ha−1 yr−1 (Slight), 10 – 20 t ha−1 yr−1 (Moderate), 20 – 40 t ha−1 yr−1 (Moderate high), 40 – 80 t ha−1 yr−1 (Severe) and more than 80 t ha−1 yr−1 (Very severe) (Singh *et al*., 1992).

Once the annual rate of soil erosion is estimated for the entire study area, the priority areas of conservation were identified at the village level. The village boundary was derived from the Socioeconomic Data and Application Centre (SEDAC) and was extracted according to the study area in ArcGIS software. Using zonal statistics in the Spatial Analyst extension in Arc Toolbox, the mean soil loss value for each village was estimated from the soil erosion estimation map. The villages were later reclassified into six priority classes ranging from high to low mean soil erosion value.

RESULTS AND DISCUSSION

Rainfall erosivity factor (R)

The force of raindrops and consequent surface soil erosion of any region is the outcome of precipitation and sediment yield (Duarte *et al*., 2016). The annual average rainfall (1981- 2022) in the Majuli District ranged from 2382.86 to 2842.79 mm (Fig. 3. a) which was very high compared to other parts of India. About 38 % (372.33 sq. km) of the area receives average rainfall between 2382.86 to 2563.23 mm and the remaining 62 % (597.79 sq. km) area receives rainfall ranging between 2563.23 to 2842.79 mm. The rainfall erosivity R factor derived using eq. 1 ranges between

1110.94 to 943.98 MJ mm ha^{-1} h^{-1} yr^{-1} (Fig. 3. b). The higher rainfall and K factor value was witnessed in the study area's northern and central parts and the lowest value was seen in the south-eastern part in and around the Brahmaputra River channel.

Soil Erodibility factor (K)

The main soil types of the study area consisted of Acrisols, Cambisols, Fluvisols, Gleysols, Luvisols and Vertisols. Cambisols (highly weathered younger alluvium) was the dominant soil type spread across 59 % (574.95 sq. km) of the area followed by Acrisols 19 % (185.45 sq. km), Fluvisols 18.6 % (181.11 sq. km), Gleysols 2.83 % (27.49 sq. km) and the remaining was shared by Luvisols and Vertisols roughly 1% (0.85 sq. km) (Fig. 4. a). The results of soil erodibility K factor generated using eq. 3 ranged between 0.0233 to 0.0154 h MJ^{-1} mm^{-1} (Fig. 4. b). Since, K factor value closer to 0 indicates that the soil is less prone to erosion and a value closer to 1 indicates weaker soil with higher rate of soil erosion, Fluvisols with a K value of 0.0233 MJ^{-1} mm^{-1} were most severely affected by soil erosion while Luvisols with a K value of 0.0154 MJ^{-1} mm^{-1} was found to be least susceptible to soil erosion (Table 2).

Slope length and Steepness factor (LS)

The LS factor plays an important role in the process of soil erosion (Mohapatra, 2022). The slope map generated using SRTM DEM data provided the topographic

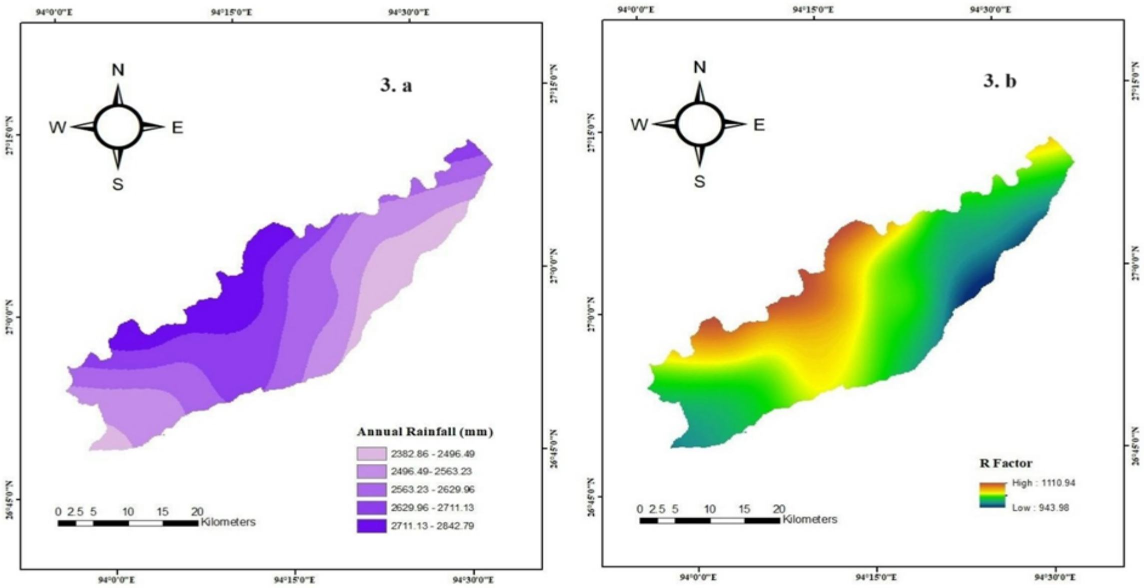

Fig. 3. *(a) Average Annual rainfall 1981-2022; (b). R factor map*

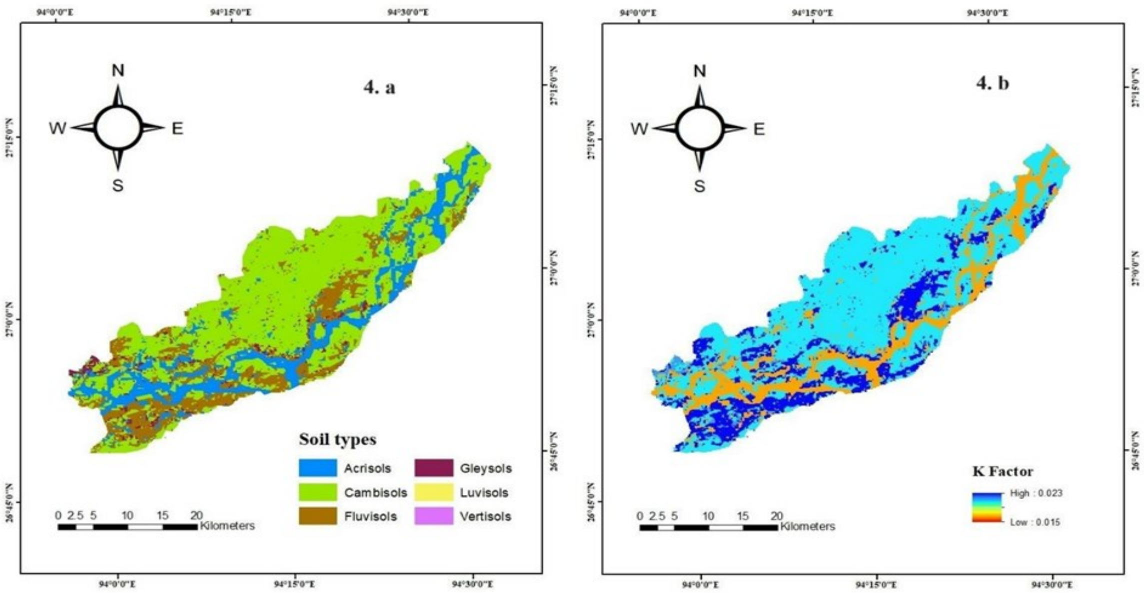

Fig. 4. *(a) Major Soil types; (b). K factor map*

Table 2. Soil properties and the values of ƒcs and, ƒcl-si, ƒorgC and ƒhisand and K factor of the study area.

Soil Type	Sand (%)	Clay (%)	Silt (%)	Organic Carbon (%)	fcsand	fcl-si	Forgc	fhisand	K Factor
Acrisols	49.0	24.0000	27.0000	1.0000	0.2000	0.8263	0.9919	0.9993	0.0216
Cambisols	42.0	22.0000	36.0000	1.0000	0.2003	0.8667	0.9919	0.9998	0.0227
Fluvisols	39.0	20.0000	41.0000	0.9000	0.2008	0.8876	0.9939	0.9999	0.0233
Gleysols	40.0	21.0000	39.0000	1.2500	0.2006	0.8788	0.9860	0.9999	0.0229
Luvisols	81.0	10.0000	9.0000	0.5700	0.2000	0.7992	0.9982	0.7360	0.0155
Vertisols	16.0	55.0000	29.0000	0.7500	0.2164	0.7268	0.9964	1.0000	0.0206

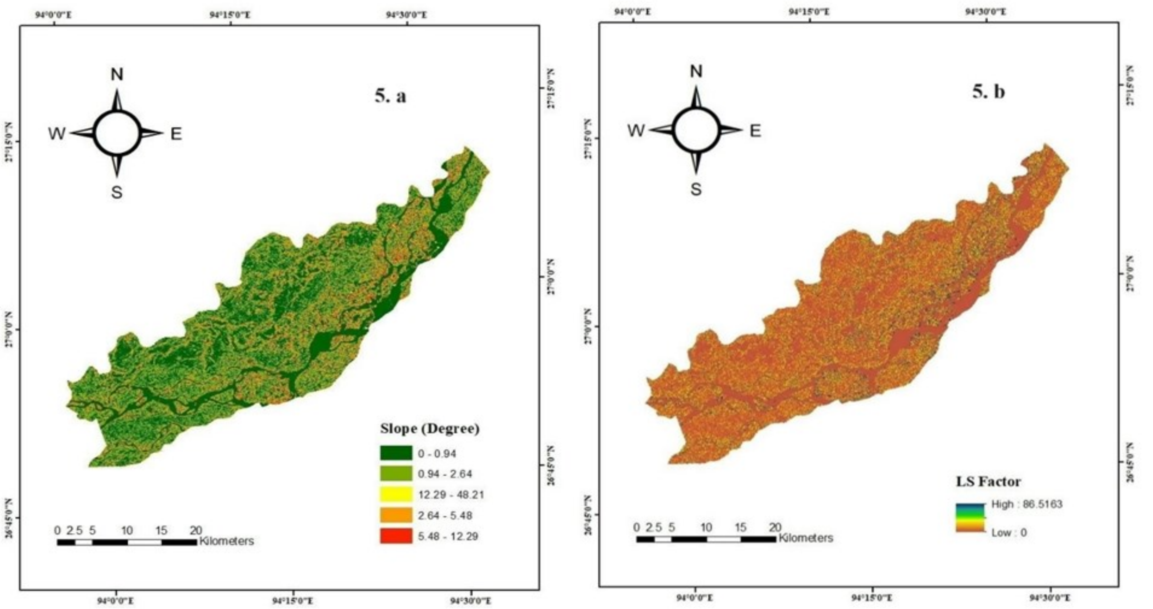

Fig. 5. *(a) Slope in degrees; (b). LS factor map*

information of the study area. The slope ranged between 0 to 48.21 degrees (Fig. 5. a), where 45. 65% (459.63 sq. km) fell under the category of 0– 0.94 degrees slope, 0.94 – 2.64 degrees slope contributed 35.45 % (356.92 sq. km), 2.64 – 5.48 degree slope accounted for 15.52 % (156.30 sq. km) and the remaining 3.37% (33.68 sq. km) area was dominated by 5.48 to 48.21-degree slope angle.

The LS factor generated using eq. 8 in the ArcGIS environment showed that the value ranged between 0 to 86.51 (Fig 5. b). It was observed that when slope and flow accumulation increased, the LS factor also increased. Brahmaputra River channel had the lowest LS factor value as the area is a flat surface whereas, stream banks and undulating slope associated with the settlement area had the highest LS value.

Cover Management (C) and Practice (P) factor

The land use and land cover were classified from the Landsat 8 imageries with the help of a supervised classification technique using maximum likelihood algorithms (Fig. 6. a). The study area presented different LULC classes namely, Dense vegetation, water bodies, sand dunes, built-up areas, Agricultural land (wet-paddy cultivation), and barren land. Almost 35% of the study area (346.83 sq. km) was covered by agricultural field where paddy cultivation dominated and dense vegetation was scattered in the central and northern parts of the region occupying the least area roughly, 0.67 % (6.513 sq. km). The C factor value (Fig. 6. b) was assigned to different LULC classes, the highest value of 1 was provided to Built-up, sand dune, and barren land as these areas were found to be without cover management, waterbodies were assigned 0 value, dense vegetation (0.004) and agricultural land (0.28) following several literatures (United States Soil Conservation Service, 1972; Wischmeier and Smith, 1978; Pandey *et al*., 2007). The P factor value (Fig. 6. c) indicated the erosion-resistant practices in the study area. Since, the study area is generally a plain topography, no significant conservation practices were noticed, thus, the values for the P factor were assigned as 1.0 for the areas without any conservation practices namely, sand dune and barren land whereas, the rest of the

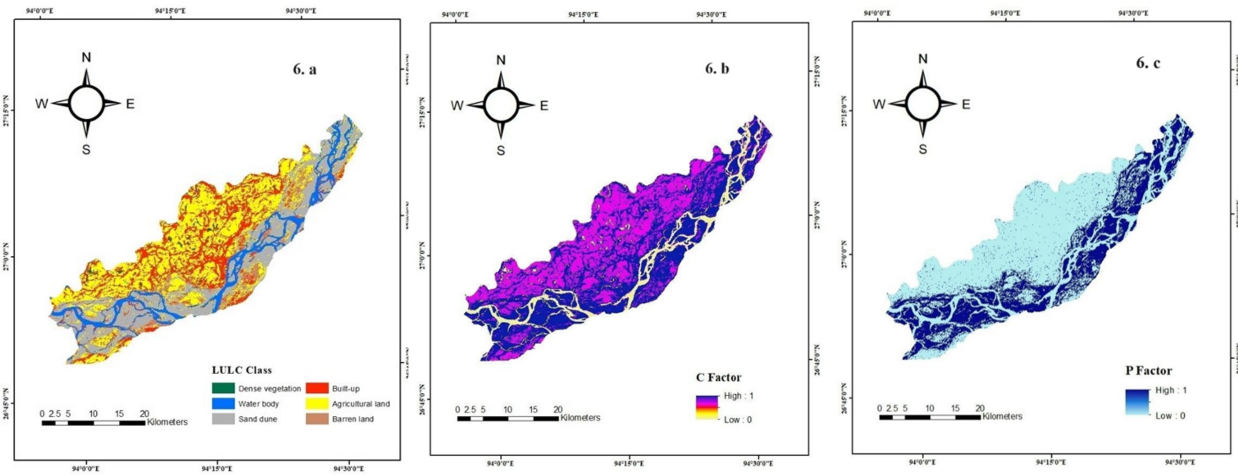

Fig. 6. *(a) Land use and land cover types; (b) C factor map; (c) P factor map*

Table 3. LULC types, their areal coverage and C and P factor value

LULC types	Area (Sq. Km)	Area (%)	C Factor	P Factor
Water body	103.798	10.699	0.000	0.000
Dense vegetation	6.513	0.671	0.004	0.000
Built-up	185.683	19.140	1.000	0.000
Sand dune	244.239	25.176	1.000	1.000
Agricultural land	346.830	35.750	0.280	0.000
Barren land	83.080	8.564	1.000	1.000

areas providing minimum support practices were assigned a value of 0 (Dabral *et al*., 2008; Pandey *et al*., 2007; Zonunsanga, 2016). Table 3. Shows different land use and land cover types and their assigned C and P values.

Potential soil loss at Majuli Island

The soil erosion severity of the study area was estimated using eq. 1 overlaying the thematic layers namely, R, K, LS, C, and P factors in the ArcGIS environment. The average annual soil loss ranged from 0 to 711 t ha^{-1} yr^{-1}, with a mean annual loss of 23.02 t ha^{-1} yr^{-1}. The entire study area was divided into six categories (Fig. 7. a) namely, very slight (< 5 t ha^{-1} yr^{-1}), slight (5 – 10 t ha^{-1} yr^{-1}), moderate (10 – 20 t ha^{-1} yr^{-1}), moderate-high (20 – 40 t ha^{-1} yr^{-1}), severe (40 – 80 t ha^{-1} yr^{-1}) and very severe (> 80 t ha^{-1} yr^{-1}). A large portion of the study area was classified into a very slight soil erosion category, accounting for more than 90 % (861.164 sq. km). These areas were dominated by paddy cultivation, built-up areas on a relatively higher slope. Very severe soil erosion covered 0.691 sq. km (0.072%) of the area, and severe soil erosion covered nearly 0.3% (2.63 sq. km) of the area. These areas were mostly noticed in some isolated pockets on the immediate northern bank of the river Brahmaputra. The sinuous curve generated by the river channel due to its northward shift in these places and the presence of barren land and sand dunes devoid of any support practices were responsible for the very high rate of soil erosion. The results also revealed that more than 5% of the study area fell under slight soil erosion categories, which was roughly 50 sq. km. More than 3% (30.63 sq. km) fell under the moderate category and roughly 1% (10.78 sq. km) fell under the moderate high soil erosion category (Table 4).

Identification of priority areas of conservation (Village- level)

Soil erosion conservation is a tedious process requiring a lot of time, money, and effort. Due to these reasons, it cannot be implemented all over the study area at the same time. Thus, the priority areas of conservation were delineated using a village-level map using zonal statistics depicting mean soil loss t ha^{-1} yr^{-1}. The entire villages in Majuli district were classified into six categories (Fig. 7. b) based on their priority level for conservation planning namely, Priority level 1 (< 7.090 mean soil loss t ha^{-1} yr^{-1}), priority level 2 (3.807 – 7.090 mean soil loss t ha^{-1} yr^{-1}), priority level 3 (2.483 – 3.807 mean soil loss t ha^{-1} yr^{-1}), priority level 4 (1.517 – 2.483 mean soil loss t ha^{-1} yr^{-1}), priority level 5 (0.721 – 1.517 mean soil loss t ha^{-1} yr^{-1}) and priority level 6 (> 0.721 mean soil loss t ha^{-1} yr^{-1}). The study revealed that out of 245 villages (cadastral and non-cadastral), 1 village fell under priority zone I, 18 villages

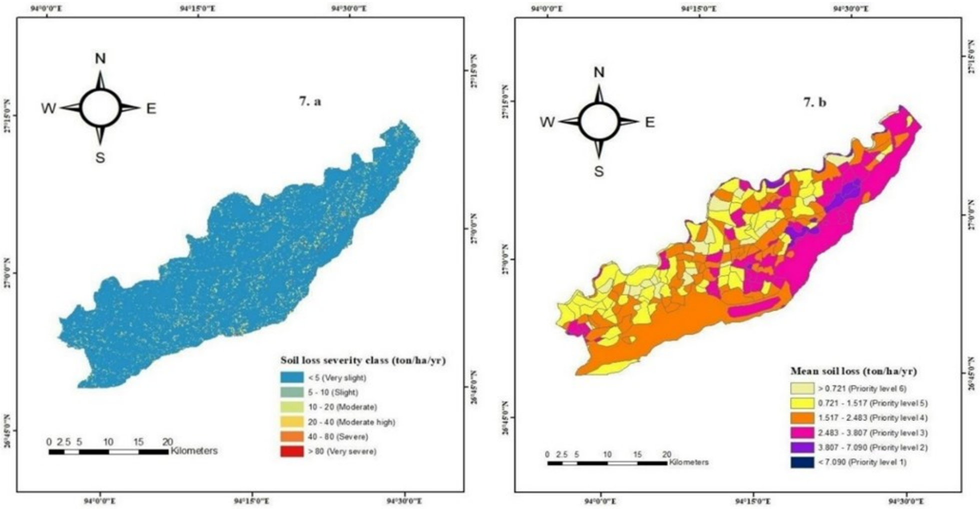

Fig. 7. *(a) Soil loss severity map; (b) Village-level Mean soil loss map*

fell under priority zone II, 52 villages were identified as priority zone III, 72 village fell under priority zone IV, 60 villages were identified as priority zone V and 42 villages were considered least affected by soil erosion and were delineated as priority zone VI (Table 5). The overall estimation of soil erosion in Majuli Island using the RUSLE model suggested that most of the study area had low soil erosion susceptibility, whereas, the region nearby by the river banks (barren and sandy areas) were most severely affected by soil erosion and required protection at highest priority (Fig. 8).

Table 4. Soil erosion severity classes and their areal coverage.

Severity classes	Area (sq. km)	% Area
< 5 (Very slight)	861.164	90.090
5 - 10 (Slight)	50.003	5.231
10 - 20 (Moderate)	30.629	3.204
20 - 40 (Moderate high)	10.780	1.128
40 - 80 (Severe)	2.628	0.275
> 80 (Very severe)	0.691	0.072

Conclusion

The soil erosion estimation for Majuli Island was carried out using the RUSLE model integrated with remote sensing and GIS techniques. The model considered five parameters namely, Rainfall erosivity factor (R), Soil Erodibility Factor (K), Slope Length and Steepness Factor (LS), Cover Management (C), and Practice (P) factor for the identification of soil erosion severity zones. The results revealed that most of the study area (more than 90%) had a very slight rate of soil erosion, which roughly accounted for less than 5 t ha^{-1} yr^{-1}. Several small pockets near the river banks exhibited severe soil erosion, accounting for 40 – 711 t ha^{-1} yr^{-1}. The study also delineated priority conservation areas by identifying villages affected by soil erosion at various scales. It was found that out of 245 villages, 1 village falls under priority level I and requires immediate attention, priority level II had 18 villages where conservation strategies are to be adopted, priority level III contains 52 villages, priority level IV included 72 villages, priority level V encompasses 60 villages and rest 42 villages were identified as priority level VI. These villages have comparatively lesser erosion severity, but effective planning and conservation efforts will be necessary to protect against soil erosion in the long run. Thus, it can be stated that the RUSLE model proves to be very effective in predicting the rate of soil erosion in the study area, but the accuracy of such prediction could only be assured with the help of numerical data derived from monitoring stations and previous studies, which is

Table 5. Village-level priority areas of conservation and aggregate mean soil erosion rate

Priority level	Sum of Mean Soil erosion rate (t ha−1 yr−1)	Sum of Area (Hectares)	No. of Villages
I	23.0167	10.585	1
II	87.872	3519.014	18
III	152.812	27884.271	52
IV	144.14	24379.927	72
V	66.261	24054.324	60
VI	14.544	6794.5162	42
Grand Total	488.647	86642.637	245

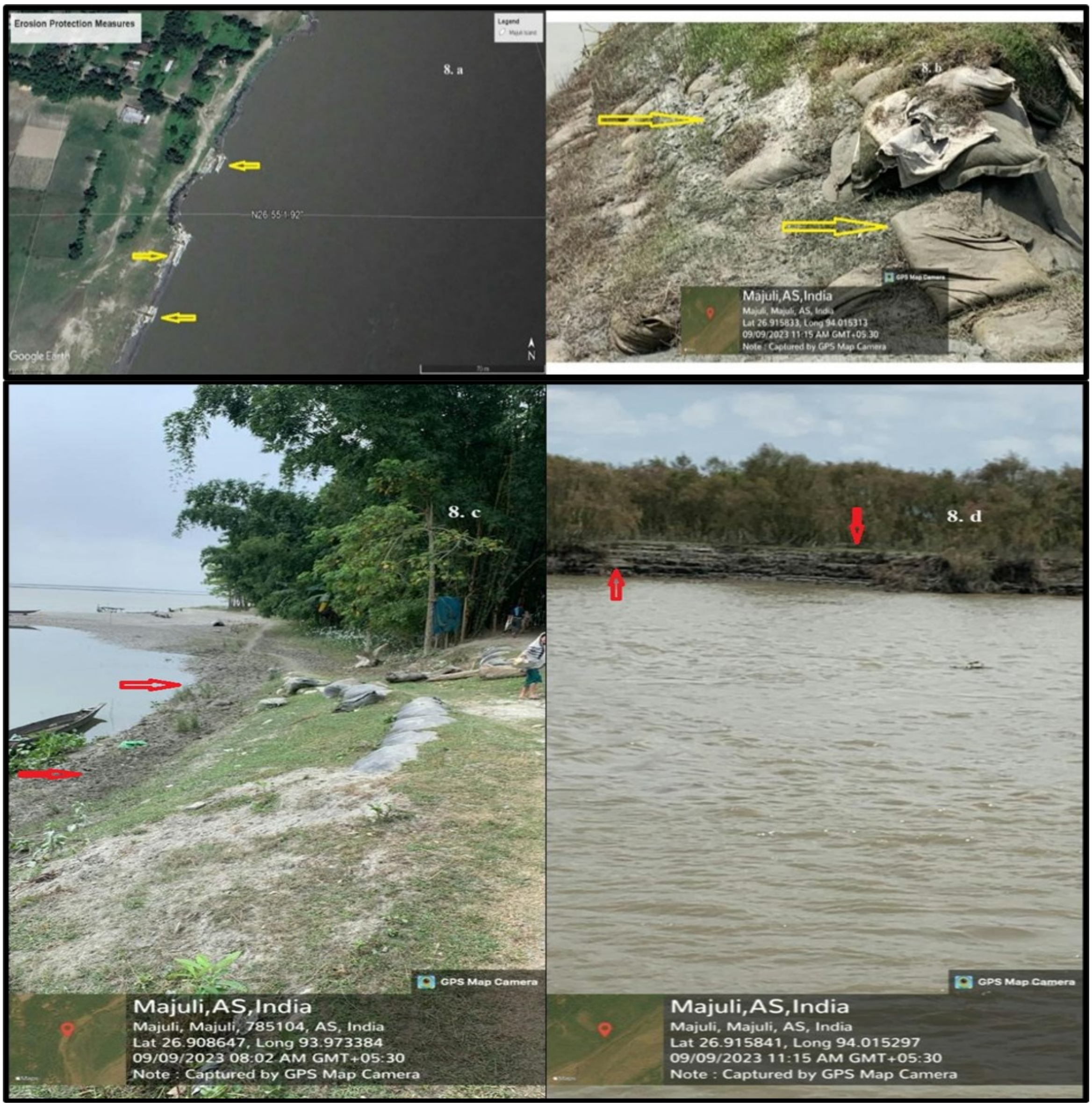

Fig. 8. *(a) Satellite image of embankments on riverbank; (b) Damage of embankments due to severe erosion; (c) Severe soil erosional site; (d) Riverbank protection measures*

absent in the case of Majuli river Island. Proper soil loss management will be possible with more intensive and gradual research in the present study area. This research will serve as a repository of information for managing and conserving soil resources vulnerable to erosion.

ACKNOWLEDGEMENTS

The authors express their profound gratitude to Virendar Singh and Kamal Das for assisting in field visits. The authors highly acknowledge the Department of Geography, Rajiv Gandhi University and the Centre for Studies in Geography, Dibrugarh University, for their kind support and encouragement.

Conflict of interest

The authors declare that they have no conflict of interest.

REFERENCES

1. Ayalew, D. A., Deumlich, D., Šarapatka, B. & Doktor, D. (2020). Quantifying the sensitivity of NDVI-based C factor estimation and potential soil erosion prediction using Spaceborne earth observation data. *Remote Sensing*. 12 (7), 1136. doi.org/10.3390/rs12071136
2. Barman, B. K., Rao, K. S., Sonowal, K., Prasad, N. S. R. & Sahoo, U. K. (2020). Soil erosion assessment using revised universal soil loss equation model and geo-spatial technology: A case study of upper Tuirial river basin, Mizoram, India. *AIMS Geosciences*, *6*(4), 525-545. https://doi.org/10.3934/geosci.2020030
3. Batjes, N. H., Ribeiro, E. & van Oostrum, A. (2020).Standardised soil profile data to support global mapping and modelling (WoSIS snapshot 2019). *Earth Syst. Sci. Data*, 12, 299–320. doi.org/10.5194/essd-12-299-2020

4. Benkobi, L., Trlica, M. & Smith, J. (1994). Evaluation of a redefined surface cover sub-factor for use in RUSLE. *Journal of Range Management*, 47, 74–78. http://dx.doi.org/10.2307/4002845
5. Bhattacharyya, R., Ghosh, B. N., Mishra, P. K., Mandal, B., Rao, C. S., Sarkar, D., Das, K., Anil, K. S., Lalitha, M., Hati, K. M. & Franzluebbers, A. J. (2015). Soil degradation in India: Challenges and potential solutions. *Sustainability*, 7(4), 3528–3570. https://doi.org/10.3390/su7043528
6. Bhattarai, R. & Dutta, D. (2007). Estimation of soil erosion and sediment yield using GIS at catchment scale. Water Res Manage. 21(10),1635–1647. doi.org/10.1007/s11269-006-9118-z
7. Bhatt, B. P., Mondal, S., Saurabh, K., Naik, S. K., Rao, K. K., & Ahmed, A. (2020). Soil Health and Fertilizer Use in India. In: Soil and Fertilizers (pp. 183-207). CRC Press
8. Biggelaar, C. D., Lal, R., Eswaran, H., Breneman, V. E. & Reich, P. F. (2003). Crop yield losses to soil erosion at regional and global scales: evidence from plot-level and GIS data. In: Land quality, agricultural productivity, and food security: Biophysical processes and economic choices at local, regional, and global levels, (pp 262-279). Edward Elgar Publishing Ltd, United Kingdom
9. Buraka, T., Elias, E., Suryabhagavan, V.K. & Lelago, A. (2022). Assessment of soil erosion risks in response to land-use and land-cover changes in Coka watershed, Southern Ethiopia. *Geology, Ecology, and Landscapes*. https://doi.org/10.1080/24749508.2022.2109825
10. Chang, T.J., Zhou, H. & Guan, Y. (2016). Applications of Erosion Hotspots for Watershed Investigation in the Appalachian Hills of the United States. *J. Irrig. Drain Eng*, 142. doi.org/10.1061/(ASCE)IR.1943-4774.0000974
11. Dabral, P.P., Baithuri, N. & Pandey, A. (2008). Soil erosion assessment in a hilly catchment of North Eastern India using USLE, GIS and remote sensing. *Water Resource Management*, 22, 1783–1798. doi.org/10.1007/s11269-008-9253-9
12. Demirci, A. & Karaburun, A. (2012). Estimation of soil erosion using RUSLE in a GIS framework: a case study in the Buyukcekmece Lake watershed, northwest Turkey. *Environ Earth Sci*. 66(3), 903–913. doi.org/10.1007/s12665-011-1300-9
13. *Ditzler, C., Scheffe, K. & Monger, H.C. (1951).* Soil Survey Manual. In: Soil Conservation Service, Soil Survey Staff, U.S. Dept. of Agricultural handbook 18, (p 503). U.S. Govt. Print Office, Washington D.C., USA
14. Duarte, L., Teodoro, A.C., Gonçalves, J.A., Soares, D. & Cunha, M. (2016). Assessing soil erosion risk using RUSLE through a GIS open-source desktop and web application. *Environ Monit Assess*, 188, 351 doi.org/10.1007/s10661-016-5349-5
15. Dutta, M. K., Barman, S. & Aggarwal, S. P. (2010). A study of erosion-deposition processes around Majuli Island, Assam. *Earth Science India*, 3 (4), 206-216
16. Food and Agriculture Organization (2019). Proceedings of the Global Symposium on Soil Erosion. Outcome Document. Retrieved from https://www.fao.org/3/ca5582en/CA5582EN
17. Erencin, Z. (2000). C-Factor Mapping Using Remote Sensing and GIS; A case Study of Lom Sak/Lom Kao, Thailand. International Institute for Aerospace Survey and Earth Sciences (ITC): Upper Aise, The Netherlands. Retrieved July 31, 2023, http://geb.uni-giessen.de/geb/volltexte/2004/1537/
18. Fu, B.J., Zhao, W.W., Chen. L.D., Zhang, Q.J., Lü, Y.H., Gulinck, H. & Poesen, J. (2005). Assessment of soil erosion at large watershed scale using RUSLE and GIS: a case study in the Loess Plateau of China. *Land Degrad Dev*. 16(1), 73–85. doi.org/10.1002/ldr.646
19. Ganasri, B. P. & Ramesh, H. (2016). Assessment of soil erosion by RUSLE model using remote sensing and GIS-A case study of Nethravathi Basin. *Geoscience Frontiers*, 7(6), 953-961. doi.org/10.1016/j.gsf.2015.10.007
20. Ghosal, K.& Das Bhattacharya, S. (2020). A Review of RUSLE Model. *J Indian Soc Remote Sens***,** 48, 689–707. doi.org/10.1007/s12524-019-01097-0
21. Ghosh, A., Rakshit, S., Tikle, S., Das, S., Chatterjee, U., Pande, C. B., Alataway, A., Al-Othman, A. A., Dewidar, A. Z. & Mattar, M. A. (2022). Integration of GIS and Remote Sensing with RUSLE Model for Estimation of Soil Erosion. *Land*, *12*(1), 116. https://doi.org/10.3390/land12010116
22. Goswami, R. (2011). Arsenic in the groundwater of Majuli-the largest river island of the Brahmaputra: prevalence, exposure impacts and removal using a novel nano adsorbent. Department of Environmental Science, Tezpur University. Retrieved from http://hdl.handle.net/10603/99696
23. Groenendyk, D.G., Ferre, T.A., Thorp, K.R. & Rice, A.K. (2015). Hydrologic-process-based soil texture classifications for improved visualization of landscape function. *PLoS One*. 10(6),1-17. doi.org/10.1371/journal.pone.0131299
24. Guo, Y., Peng, C., Zhu, Q., Wang, M., Wang, H., Peng, S., & He, H. (2019). Modelling the impacts of climate and land use changes on soil water erosion: Model applications, limitations, and future challenges. *Journal of Environmental Management*, 250, 109403. https://doi.org/10.1016/j.jenvman.2019.109403
25. Issaka, S. & Ashraf, M. A. (2017). Impact of soil erosion and degradation on water quality: a review. *Geology, Ecology and Landscapes*. 1(1), 1-11. DOI: 10.1080/24749508.2017.1301053
26. Jamal, S., Ahmad, W. S., Ajmal, U., Aaquib, M., Ali, M.A., Ali, M.B. & Ahmed, S. (2022). An integrated approach for determining the anthropogenic stress responsible for degradation of a Ramsar Site-Wular Lake in Kashmir, India". *Marine Geodesy*, 45(4), 407-434. https://doi.org/10.1080/01490419.2022.2034686
27. Jiang, L., Yao, Z., Liu, Z., Wu, S., Wang, R. & Wang, L. (2015). Estimation of soil erosion in some sections of Lower Jinsha River based on RUSLE. *Nat Hazards*. 76 (3),1831–1847. https://doi.org/10.1007/ s11069-014-1569-6.
28. Karamage, F., Zhang, C., Liu, T., Maganda, A. & Isabwe, A. (2017). Soil erosion risk assessment in Uganda. *Forests*. 8(2),1–20. doi.org/10.3390/f8020052
29. Kouli, M., Soupios, P. & Vallianatos, F. (2009). Soil erosion prediction using the Revised Universal Soil Loss Equation (RUSLE) in a GIS framework, Chania, Northwestern Crete. *Greece Environ Geol.* 57(3), 483–497. doi.org/10.1007/s00254-008-1318-9
30. Makhdumi, W., Shwetha, H.R. & Dwarakish, G.S. (2023). Soil erosion in diverse agroecological regions of India: a comprehensive review of USLE-based model-

ing. *Environmental Monitoring and Assessment*, 195, 1112. https://doi.org/10.1007/s10661-023-11687-8

31. Meiyappan, P., Roy, P. S.,Soliman, A., Li, T., Mondal, P., Wang, S. &Jain, A. K. (2018). India Village-Level Geospatial Socio-Economic Data Set: 1991, 2001. Palisades, New York: NASA Socioeconomic Data and Applications Center (SEDAC). Retrived on July, 16, 2023, doi.org/10.7927/H4CN71ZJ
32. Mohapatra, R. (2022). Application of revised universal soil loss equation model for assessment of soil erosion and prioritization of ravine infested sub basins of a semi-arid river system in India. *Model. Earth Syst. Environ*, 8, 4883–4896. doi.org/10.1007/s40808-022-01388-5
33. Pandey, A., Chowdary, V. M. & Mal, B. C. (2007). Identification of critical erosion prone areas in the small agricultural watershed using USLE, GIS and remote sensing. *Water resources management*, 21, 729-746. doi.org/10.1007/s11269-006-9061-z
34. Parysow, P.; Wang, G.X., Gartner, G.& Anderson, A.B. (2003). Spatial uncertainty analysis for mapping soil erodibility based on joint sequential simulation. *Catena*, 53, 65–78. doi.org/10.1016/S0341-8162(02)00198-4
35. Pham, T. G., Degener, J. & Kappas, M. (2018). Integrated universal soil loss equation (USLE) and Geographical Information System (GIS) for soil erosion estimation in A Sap basin: Central Vietnam. *International Soil and Water Conservation Research*, 6 (2), 99-110. doi.org/10.1016/j.iswcr.2018.01.001
36. Rajbanshi, J. & Bhattacharya, S. (2020). Assessment of soil erosion, sediment yield and basin specific controlling factors using RUSLE-SDR and PLSR approach in Konar river basin, India. *Journal of Hydrology*, 587, 124935. https://doi.org/10.1016/j.jhydrol.2020.124935
37. Renard, K.G., Foster, G.R., Weesies, G.A., McCool, D.K. & Yoder, D.C. (1996). Predicting soil erosion by water: a guide to conservation planning with the Revised Universal Soil Loss Equation (RUSLE). In: Agriculture Handbook 703, (p 25–28), Washington DC, USA
38. Renard, K.G., Foster, G., Weesies, G., McCool, D. & Yoder, D. (1997). Predicting Soil Erosion by Water: A Guide to Conservation Planning with the Revised Universal Soil Loss Equation (Rusle). Agriculture Handbook No.703, (pp 404). United States Government Printing, United States Department of Agriculture, Washington, DC, USA.
39. Sankhua, R. N., Sharma, N., Garg, P. K. & Pandey, A. D. (2005). Use of remote sensing and ANN in assessment of erosion activities in Majuli, the world's largest river island. *International Journal of Remote Sensing*. 26 (20), 4445-4454. doi.org/10.1080/01431160500185474
40. Schwab, G. O., Fangmeier, D. D., Elliot, W. J., Frevert, R. K. & Leonard, R. A. (1994). Soil and water conservation engineering. *Journal of Environmental Quality*, *23*(2), 390. doi.org/10.1017/S0021859600068611
41. Sharpley, A.N. & Williams, J.R. (1990). Erosion/Productivity Impact Calculator: 1. Model Documentation. In: Technical bulletin, 1768 (235), US Department of Agriculture. Washington DC, USA
42. Singh, G., Babu, R., Narain, P., Bhushan, L. S. & Abrol, I. P. (1992). Soil erosion rates in India. *Journal of Soil and water Conservation*, 47(1), 97-99
43. Srinivas, C.V., Maji, A.K., Obi Reddy GP. & Chary, G.R. (2002). Assessment of soil erosion using remote sensing and GIS in Nagpur district, Maharashtra for prioritisation and delineation of conservation units. *Journal of the Indian Society of Remote Sensing*. 30(4),197–212. doi.org/10.1007/BF03000363
44. Sujatha, E. & Sridhar, V. (2018). Spatial Prediction of Erosion Risk of a Small Mountainous Watershed Using RUSLE: A Case-Study of the Palar Sub-Watershed in Kodaikanal, South India. *Water*. 10 (11), 1608. doi.org/10.3390/w10111608
45. United States, (1972). SCS National Engineering Handbook, section 4. Hydrology. Govt. Print. Off. United States Department of Agriculture, Washington DC, USA
46. Wischmeier, W. & Smith, D. (1957). Factors affecting sheet and rill erosion. Transactions. *American Geophysical Union*, 38(6), 889–896. https://doi.org/10.1029/TR038i006p00889
47. Wischmeier, W. H. & Smith, D. D. (1978). Predicting rainfall erosion losses: a guide to conservation planning. Agriculture Handbook No. 537. United States Government Printing, Department of Agriculture, Science, and Education Administration, Wahington, DC, USA
48. Yue-Qing, X., Xiao-Mei, S., Xiang-Bin, K., Jian, P. & Yun-Long, C. (2008). Adapting the RUSLE and GIS to model soil erosion risk in a mountains karst watershed, Guizhou Province, China. *Environ Monit Assess*. 141(1), 275– 286. doi.org/10.1007/s10661-007-9894-9
49. Zhao, J., Yang, Z. & Govers, G. (2019). Soil and water conservation measures reduce soil and water losses in China but not down to background levels: evidence from erosion plot data. *Geoderma*, 337, 729-741. https://doi.org/10.1016/j.geoderma.2018.10.023
50. Zonunsanga, R. (2016), Estimation of Soil loss in Teirei watershed of Mizoram by using the USLE Model. *Sci Technol J* 4, 43–47. https://doi.org/10.22232/stj.2016.04.01.06